

Analysis of the effect of fluvial and tidal sediment fluxes on bifurcations in river channel networks



Rick Jankowski – 6579744

06-08-2021

MSc Thesis Earth, Surface & Water

Utrecht University – Faculty of Geosciences – Department of Physical Geography

Supervisors:

1st: dr. ir. Jaap Nienhuis

2nd: prof. dr. Steven de Jong



Utrecht University

Abstract

River deltas are complex areas with intricate channel patterns that deliver water and sediment from source to the coast. The shape and pattern of a delta or river network is prone to changes originating from sediment fluxes of fluvial and tidal origin. These changes can be devastating for the 24% of the world population living in delta areas. Quantification of the influence of these fluvial and tidal sediment fluxes on river channel networks is lacking and a global dataset on distributary networks does not yet exist. In this study, the objective is to identify relationships between delta channel networks and fluvial and tidal sediment fluxes for seven deltas around the world. A river network is derived from the JRC Global Water dataset together with the MERIT Hydro dataset available on the Google Earth Engine platform. The network is used to find the number of bifurcations, river outlets and channel lengths. All rivers are placed on a spectrum from highly fluvial dominated to highly tidal dominated and analysed based on the number of bifurcations, river outlets and channel lengths their place on the spectrum. The study finds that terminal channel length decreases with increasing tidal influence which suggests a decrease in number of bifurcations, this is corroborated by literature. This study lays the groundwork for a global understanding of fluvial and tidal influences on delta morphology, however uncertainties lie in the sample size and vector processing. Future research can build on this research by improving the image processing and increasing the number of deltas for a more reliable result.

Key words: bifurcations, deltas, delta morphology, Google Earth Engine, distributary channel network

Contents

- Abstract 2**
- 1. Introduction..... 4**
- 2. Background..... 5**
 - 2.1 Deltas..... 5
 - 2.2 Bifurcations..... 6
 - 2.3 Bifurcation stability 8
 - 2.4 River networks..... 9
 - 2.5 Knowledge gap and problem definition 10
- 3. Methods 11**
 - 3.1 Datasets 11
 - 3.2 Image processing..... 11
 - 3.3 Vector processing..... 14
 - 3.4 Statistics..... 14
- 4. Results..... 15**
 - 4.1 Nodes..... 17
 - 4.2 Segments 17
- 5. Discussion..... 20**
 - 5.1 The effect of tidal and fluvial influence on delta morphology 20
 - 5.1.1 Nodes..... 20
 - 5.1.2 River segments 20
 - 5.2 Sensitivity 21
 - 5.3 Data quality & improvement..... 21
 - 5.4 Future research 23
- 6. Conclusion 24**
- Bibliography..... 25**
- Appendix – A Sensitivity analysis 28**
 - 1. Data without Amazon..... 28
 - 2. Data without Fly 28
 - 3. Data without Lena 29
 - 4. Data without Mississippi 29
 - 5. Data without St. Lawrence 30
 - 6. Data without Yenisei 30
 - 7. Data without Yukon..... 31

1. Introduction

Coastal regions play an important role for mankind, both socially and economically (Islam et al., 2016; Kuenzer et al., 2015) and around 24% of the human population live in these coastal regions (Islam et al., 2016). Deltas are economic centres, home to a multitude of animal species and important agricultural areas. Yet, they are prone to human and climate change (Syvitski, 2008; Fofoula-Georgiou, 2013).

Every delta is different and the river pattern on a delta is never the same. But why these different channel patterns exist is not yet fully understood. Understanding why these patterns exist and how those patterns change when boundary conditions change can be of great importance for the people living in the delta area. A river changing its course can mean that people do not have access to running water nearby, or a sudden branching of the river can mean destruction for people living in the river's path. Several studies have hypothesized that channel patterns result from wave-, tide-, or river-dominant sediment fluxes (Galloway, 1975; Xue & Galloway, 1991; Kleinhans, 2010). Other studies find that the length of river segments and the amount of bifurcations a river correlates with the amount of sediment transported by the river and tides (Edmonds & Slingerland, 2007; Leonardi et al., 2013; Tejedor et al., 2015). Most of these studies that have been conducted focused on a small number of deltas and included many manual actions. As stated, the influence of tidal and fluvial sediment on a delta is well studied, however, the influences of these factors on the topology of distributary channel networks as a whole is not yet investigated thoroughly.

This study investigates the automated quantification of river networks on a large scale and compares tidal and fluvial influences. We classify each delta on their dominant sediment flux, either fluvial or tidal, and analyse the correlation with delta morphology, such as number of river mouths and bifurcations using open source data available on the Google Earth Engine platform (Gorelick et al., 2017).

Literature relevant to the study is presented in the first section. In section two, data sources and methods will be explained. In section three, results are presented. In section four the results and methods are discussed and in section five conclusions are presented.

2. Background

In order to understand the different influences of delta controls, it is necessary to understand the general theory behind some of the most notable aspects of river morphology, which will be discussed in the first section. This section will contain a breakdown of research done on river morphology in deltas dominated by tides and fluvial sediment. Next some research methods for river morphology are summarized and the chapter is concluded with the problem definition.

2.1 Deltas

Deltas emerge where a river loses speed and deposits sediment on contact with a large waterbody such as an ocean, sea or lake. The sediment is dispersed radially with multiple lobes of sedimentation, the position of which can switch over time, making the delta or river 'move' (Roberts, 1997). The delta is a part of a larger system shown in figure 2.1. The river has its origin upstream, also called the headwater, where rain or melt water is collected in a stream downward. The headwaters usually have significant height differences which make the streams incise and cut deep V-shaped valleys. The sediment eroded by the river is transported with the stream downward. The amount of sediment eroded increases with the size of the total drainage basin. The further downstream the river goes, the more water it collects and its capacity to carry sediment grows with it. Further downward where the slopes are more gentle the river merges with different streams and forms a 'trunk' channel (Olariu & Bhattacharya, 2006). The total area from where water flows to the main channel is called the drainage basin, the size of the basin also increases the total material eroded (Carson & Kirby, 1972). Flowing downward, to maintain flow in areas with relatively low slopes the river starts to meander. The point where the river transitions from incising to depositing its sediment is the apex. The area seaward of the apex is the delta area. This area is build up out of the sediment eroded in the parts above the apex. The sediment will be deposited when the stream flow decreases when the river comes in contact with the still water body (Elliot, 1986). The deposition of fluvial sediment causes the delta to build out when the deposits reach heights so that flow cannot go over and has to flow around the sediment accumulation. The amount of sediment and the transportation of sediment by tides and waves can all have an effect on the building out of the delta and can cause multiple channels or a branching pattern.

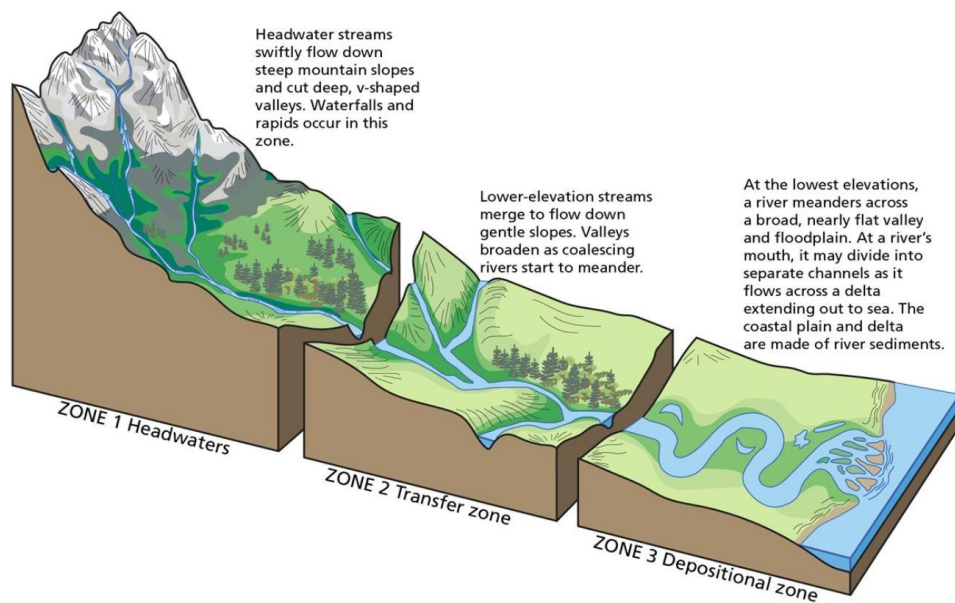


Figure 2.1. Overview of the components of a river. (source: Trista L. Thornberry-Ehrlich, Colorado State University)

2.2 Bifurcations

In a river network, streams combine on their way to the ocean into a larger stream or river (confluences). However, those rivers also have the ability to split, to bifurcate (diffluence). A bifurcation is a node where a single channel splits into two branches downstream (Kleinhans et al., 2013). Bifurcations are especially numerous in braided rivers, but also in distributary systems such as deltas. Deltas are likely to have multiple active bifurcations instead of one channel of the bifurcation being immediately abandoned (avulsion) (North & Warwick, 2007).

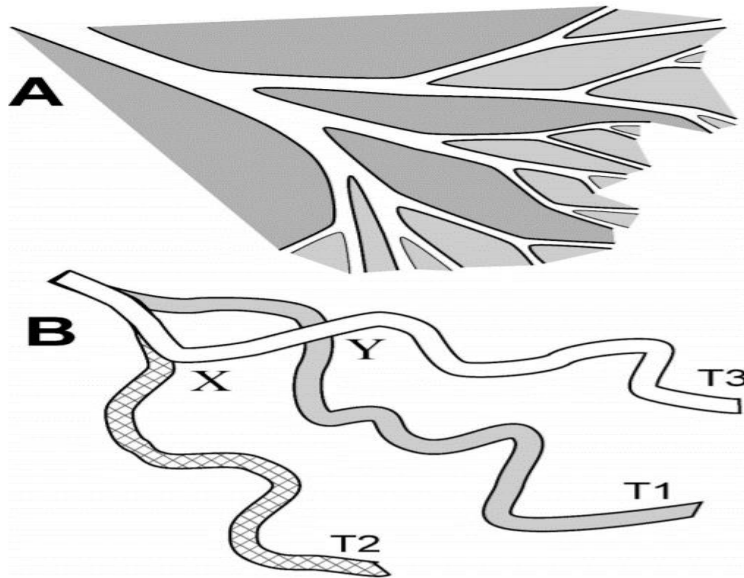


Figure 2.2. The distinction between simultaneously active channels (A) and a set of channels which are active at different points in time, first T1, then T2, then T3. (source: North & Warwick (2007))

The bifurcations shown in figure 2.2 form in two main ways: mouth-bars causing flow to split, and breaches in levees causing crevassing and thus changing the flow to a different direction (Kleinhans et al., 2013). Mouth-bar deposition take place where river channels come in contact with the sea or lake boundary. Mouth-bars form when the sediment-carrying flow or jet suddenly expands and decelerates when entering relatively still water (figure 2.3) (Bates & Freeman, 1953; Wright, 1977). They grow until the flow is directed around the bar instead of over the top of the mouth bar (figure 2.4).

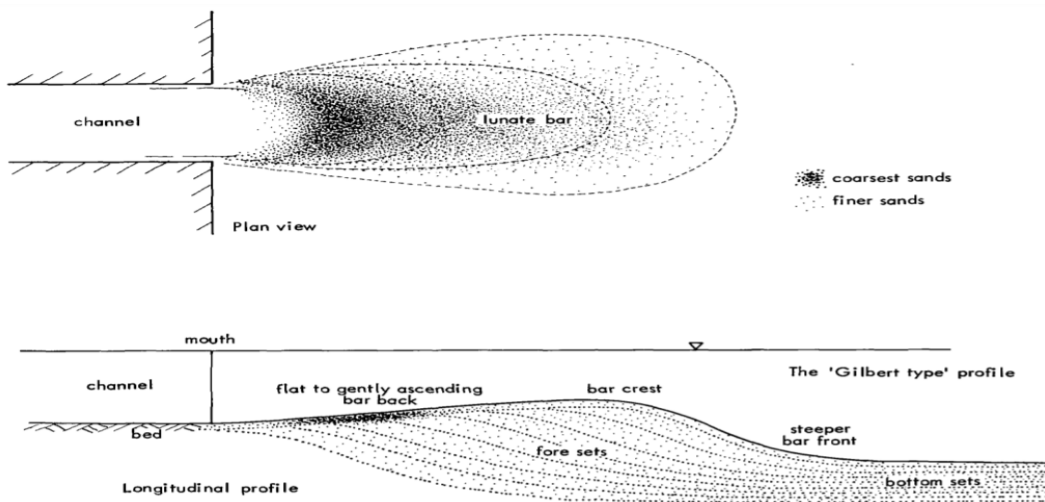


Figure 2.3. Illustration showing the idealized creation of a mouth bar in still condition in plan view (left) and longitudinal profile (right). (source: Wright, 1977)

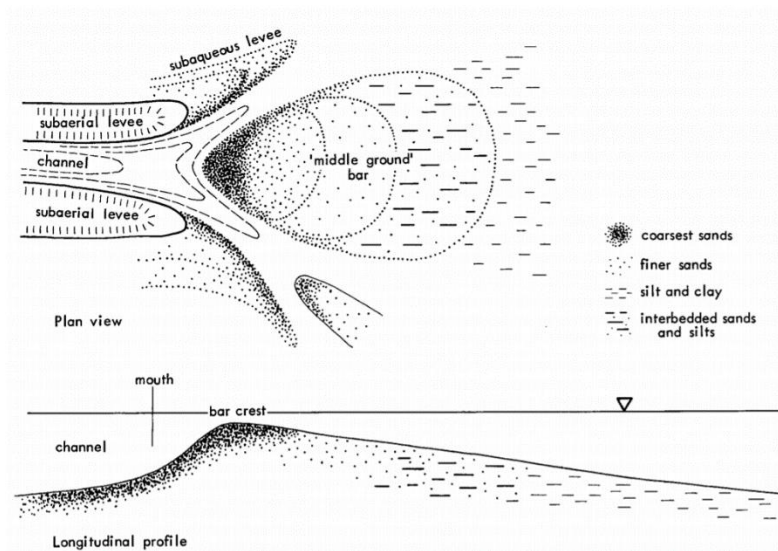


Figure 2.4. Illustration of mouth-bar forming and bifurcation in a fluvial driven delta in plan view (top) and longitudinal profile (bottom). (source: Wright, 1977)

Galloway (1975) finds that channel patterns result from varying degrees of tide-, wave- and fluvial-dominance. Galloway (1975) continues that the degree of influence affect the mouth-bar formation and sediment distribution along channels, which in turn influences the amount and formation of channels at the delta boundary. At a later stage Xue & Galloway (1991) refine this theory to include that coarseness and intensity of sediment flux also changes the susceptibility to tidal or wave influences.

A detailed analysis of this process is done in Edmonds & Slingerland (2007). They used a three dimensional model to simulate morphological evolution at the mouth of a straight channel. They found that a bar forms roughly twice the width from the channel mouth. Since the flow is divided between each bifurcation the channel width will decrease towards the delta front. This gives the delta a distinct fractal pattern shown in figure 2.5. Jerolmack & Swenson (2007) found that the channel length in such patterns are highly skewed which supports the theory. This is because the length of the river segment from the outlet to the closest bifurcation, also called the terminal channel length (Olariu & Bhattacharya, 2006) decreases with the number of bifurcations.

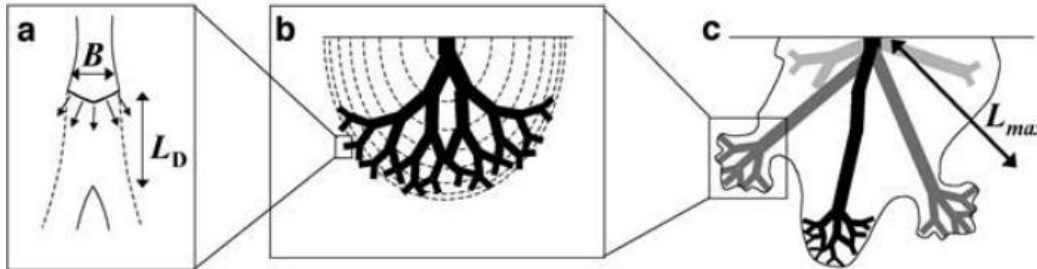


Figure 2.5. Illustration of distributary formation. a) expansion of channel flow causing a mouth-bar at length L_D . b) successive mouth-bar depositions after each bifurcation creates a branching pattern with decreasing channel length. c) On larger timescale, avulsions occur and the fractal pattern is created in a different location. (source: Jerolmack & Swenson (2007))

The downstream flow is, at the bifurcation, divided between both channels. The ratio in which this is done determines the stability of the bifurcation. An avulsion is when one of the two channels is abandoned and the flow path is shifted towards the other channel and the old channel network is abandoned (figure 2.5c). An avulsion can occur suddenly due to crevasses where the channel follows the path with the highest gradient, or gradually when one of the two channels fills with sediment due to small perturbations in the channel itself (Smith & Rogers, 1999). However, the probability of an avulsion due to height difference is quite low due to the small gradient in a deltaic environment. Any energy change can increase the chance of an avulsion or the lack thereof, such as tectonics, relative sea level change, sediment supply or backwater effect.

2.3 Bifurcation stability

The formation of mouth-bars can be influenced by several factors such as varying sediment flux by the river or tides. Kästner et al. (2017) focus on tidal influences on distributary channels. They use remote sensing and field data to try to understand the tidal influence on the Kapuas delta in Indonesia. They find that there is a general break between where the delta is predominantly influenced by incoming sediment and where the tide is most dominant. They also state that the stability of the bifurcation is determined by the the sediment flux which is in turn dependent on the tides, where the tidal wave can cause a division of sediment at the bifurcation. Distributary channels on a river-dominated system develop differently than on a tide-dominated system (Leonardi et al., 2013; Shaw & Mohrig, 2014; Iwantoro et al., 2020). Among other things, the degree to which tides change the flow at the base of the river have an important effect on delta morphodynamics such as mouth-bar formation (Wright & Coleman, 1974; Jerolmack, 2009). Leonardi et al. (2013) focus on the differences between tide-dominated and river-dominated deltas and their effects on mouth-bar formation using the Delft3D package (Roelvink & Van Banning, 1995). As mentioned in the previous paragraph and in Edmonds & Slingerland (2007), after the initial sediment is deposited in front of the channel, the mouth bar will grow until it is big enough to force the flow around the bar instead of over. When the bar reaches that height, it will widen, creating a triangular shape recognizable in illustrations above. Leonardi et al. (2013) find that tidal influence increases the spreading of the sediment near the channel mouth thus widening the mouth bar. They find that the asymmetry of flow during ebb and flood increases the flow through a central (main) channel seen as the horizontal line in figure 2.6 and predominantly in figure 2.6D, where tidal amplitude is highest. The changes in

flow prevent the central channel from filling up and deposits are formed on the sides. These deposits create bifurcations which grow with the fast flow during low tide (figure 2.6CD), a trifurcation. Since there is a main channel where much of the sediment and flow is concentrated, the side channels are not actively bifurcating, contrary to fluvial-dominated deltas. It is expected that with fluvial influence on a tidal-dominated deltas these trifurcations form. However, with low fluvial sediment flux in a tidal dominated delta the sediment will be redistributed and mouth bars take longer to form.

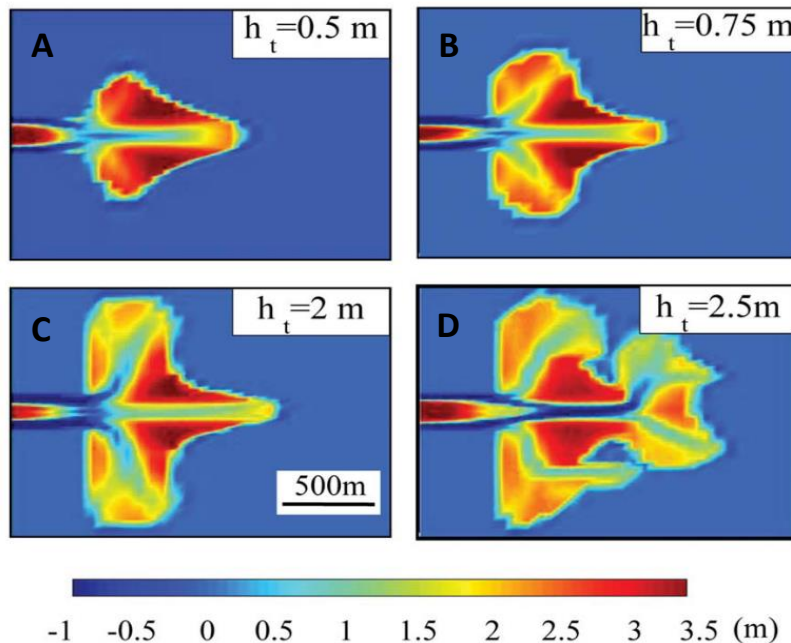


Figure 2.6. Tide-dominated delta model run for different tidal ranges, showing cumulative erosion and sedimentation for different tidal amplitudes (h_t). (source: Leonardi et al., 2013)

Tides can propagate upstream which can influence the sediment transport/erosion upstream, causing the channel not to slip up and making the bifurcation more stable (Iwantoro et al., 2020). This was investigated by using a 2D model of a single bifurcation where tidal forcing and channel geometry was varied. Iwantoro et al. (2020) say that river-dominated deltas are more unstable and prone to asymmetric sediment transport and thus unstable bifurcation channels. This can cause avulsions on a larger timescale. As mentioned earlier, the flow, as well as the sediment-load, is split between every bifurcation, this influences the creation of mouth bars as well as the influence of tides on this sediment.

2.4 River networks

A river delta is a complex environment. It has an intricate channel network which transports water and sediment all the way from the top of its catchment to the sea. To study the patterns of these networks and quantify the structure of such a network of river segments and bifurcations, a river delta needs to be seen as an object. This way the different structural elements of a river can be quantified for different degrees of tidal and fluvial influence. (Tejedor et al. (2015) constructed a framework to study delta channel network connectivity. The groundwork for this research is done by Smart & Moruzzi (1971). They divide a river into links and vertices. The vertices are split into forks (two segments into one), junctions (one segment into two) and outlets (end points) where they number each vertex in order of flow direction, also called a directed graph or graph theory. They focussed on the recombination factor (α) which is the ratio between forks and junctions. A recombination factor of 0 means there are no alternative paths from source to sink and a recombination factor of 1 would mean there are many paths. Smart & Moruzzi (1971) also try to define the different links in the river system. For this they use the connectivity matrix (figure 2.7). This is a matrix with width and length equal to the number of vertices and describes which vertices

are connected. They use this method of manipulating the matrix to find different paths from the source to coast. Tejedor et al. (2015) refine the method of Smart & Moruzzi (1971) for describing a river channel network with a connectivity matrix. They use the Laplacian of the matrix, especially the eigenvalues and eigenvectors of this Laplacian, to find the strengths and connections between nodes of the network. This method is called spectral-graph theory.

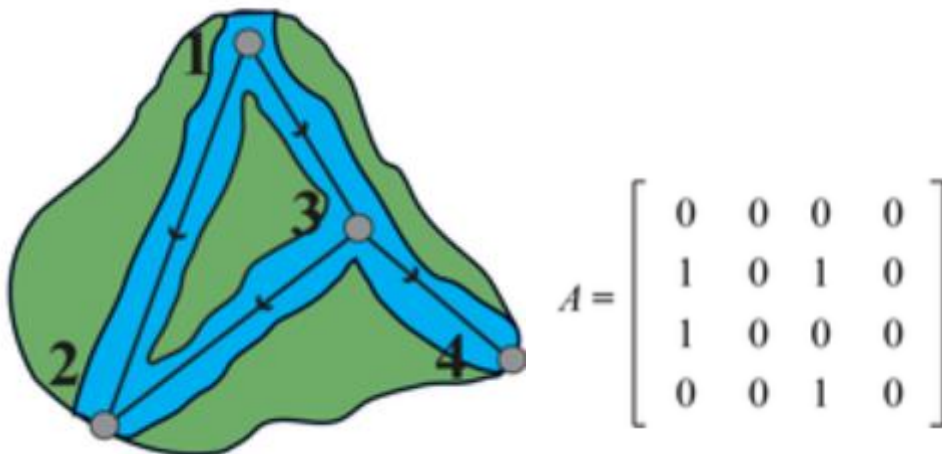


Figure 2.7. Example of a directed graph with its connectivity matrix (source: Tejedor et al., 2015)

2.5 Knowledge gap and problem definition

As stated above, the origin of a bifurcation is well studied, as well as different forces on the delta, such as tides and fluvial sediment. However, the influences of these factors on the topology of distributary channel networks as a whole is not yet investigated thoroughly. The same goes for the scale of the studies on delta forces or networks. The effect of different sediment fluxes on channel patterns has not yet been properly tested on a global scale. That is why this research focusses on quantitative research of river network topology, especially quantifying bifurcations and river mouths. The aim of this study is to gain a better understanding of tidal and fluvial influences on the river network morphology. This research tries to provide insights in how different sediment fluxes can influence channel patterns. To keep it clear, these aims are formulated in the following question and its sub questions:

What is the effect of tidal and fluvial sediment fluxes on a distributary channel network?

- 1) What influence does the ratio of fluvial and tidal sediment fluxes have on the number of bifurcations?
- 2) What influence does the ratio of fluvial and tidal sediment fluxes have on the river segments?

The main hypotheses is that with more fluvial sediment, mouth bars will grow faster and more frequently creating exponentially more bifurcations with a decreasing channel length. Tidal influence will contain this growth by creating a main channel with side channels which translates in less bifurcations and longer channel lengths.

3. Methods

This chapter describes in detail which datasets and processes are used to achieve the results discussed in the next chapter. The main goal is to go from a water occurrence image, which is available globally, to a vectorized river network where the segments and junctions can be quantified and related to fluvial and tidal sediment fluxes.

In the first section the datasets are summarized which are used in the analysis. In the next section the processes on the image layers are described followed by the processes used to transform the images to a river network where the bifurcations and river segments can be quantified. The last section describes how the channel network properties are linked to the fluvial and tidal sediment fluxes.

3.1 Datasets

For this research three datasets have been used which are available on the Google Earth Engine platform (GEE)(Gorelick et al., 2017): JRC Global Water Layers (Pekel et al., 2016), MERIT Hydro (Yamazaki et al., 2019) as well as the Large Scale International Boundaries (LSIB) dataset from the United States Office of the Geographer.

JRC Global Water Layers contain spatial and temporal data of the distribution of surface water at 30 meter resolution for the period 1984-2020, generated from the images from Landsat 5, 7 and 8. Specifically, the Occurrence Layer is used, which indicates in what percentage of the total image series each pixel contains a pixel classified as water.

MERIT Hydro is a high resolution hydrography map at 3 arc-seconds (~90 meter at the equator) developed by combining elevation data and water body datasets. Specifically the Upstream Area layer is used, which calculates for each connecting water pixel the total drainage area of the connecting waterbody.

The data of the deltas comes from Nienhuis et al. (2020), which calculates the fluvial (Q_{river}) and tidal (Q_{tide}) sediment transport for the given deltas. The deltas analysed in this research are the Amazon, Fly, Lena, Mississippi, St Lawrence, Yenisei and Yukon. Tidal sediment flux is calculated by using tidal amplitude and angular frequency extracted from the OSU TOPEX dataset (Egbert & Erofeeva, 2002). Fluvial sediment flux is calculated using the WBMSed 2.0 distributed global-scale sediment flux model (Cohen et al., 2014). Further information and analysis on the parameters can be found in the paper of Nienhuis et al. (2020).

3.2 Image processing

To extract the river from the JRC image, first a water mask is needed. To determine a mask of permanent water a threshold of 90% occurrence is set (Huang et al., 2018; Wu et al., 2019). As can be seen in figure 3.1, when filtering for permanent waterbodies, the small lakes around the river will also be taken into account.

To create connecting features out of the image the permanent water mask is run through a boundary tracing algorithm, vectorization, the results of which are shown in figure 3.2. The small lakes outside the river still show up in this result.

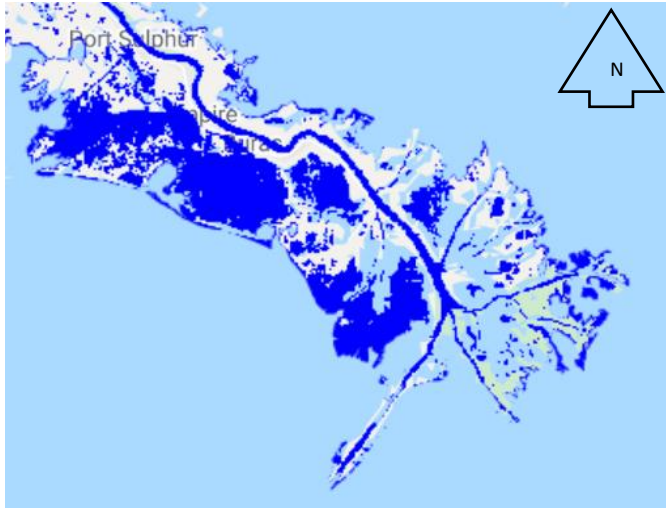


Figure 3.1. Part of the Mississippi delta with permanent water mask (occurrence $\geq 90\%$) in blue. Image from Google Earth Engine

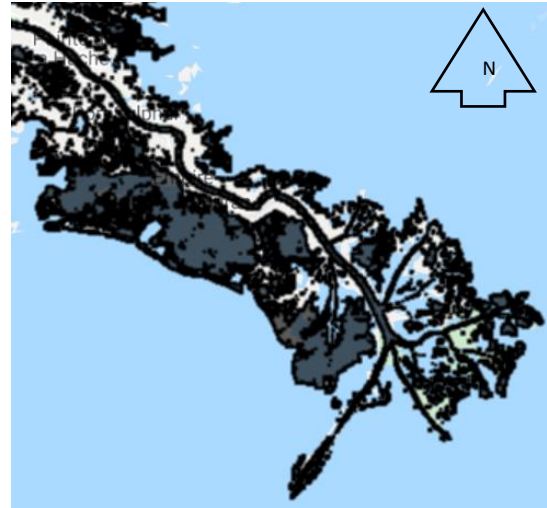


Figure 3.2. Part of the Mississippi delta with vectorized permanent water mask in black. Image from Google Earth Engine.

To filter the river from the lakes and other inland waterbodies a second image will be used, the Upstream Area layer from MERIT Hydro. From this layer all pixels except the maximum value for the upstream area is masked per delta area to extract the main river from the dataset (figure 3.3).

This result is used to extract the river from all other permanent water bodies in the permanent water mask layer. Due to the large scale operation and the limited process time of Google



Figure 3.3. Part of the Mississippi delta with the maximum upstream area in white. Image from Google Earth Engine

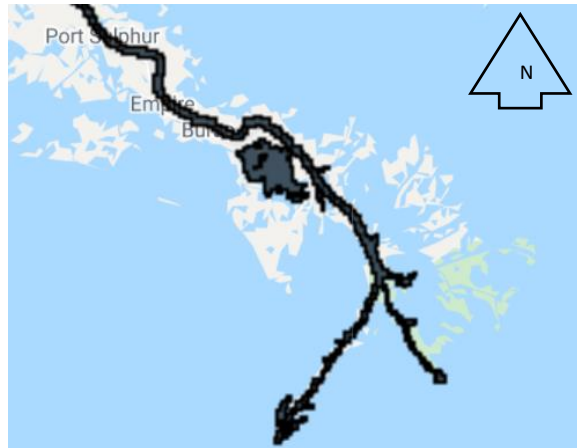


Figure 3.4. Part of the Mississippi delta with the filtered and vectorized river in black. Image from Google Earth Engine.

Earth Engine, the scale with which the JRC raster image is vectorized, is relatively small (400 meters) (figure 3.4).

A schematic overview of the image processing can be found in figure 3.5.

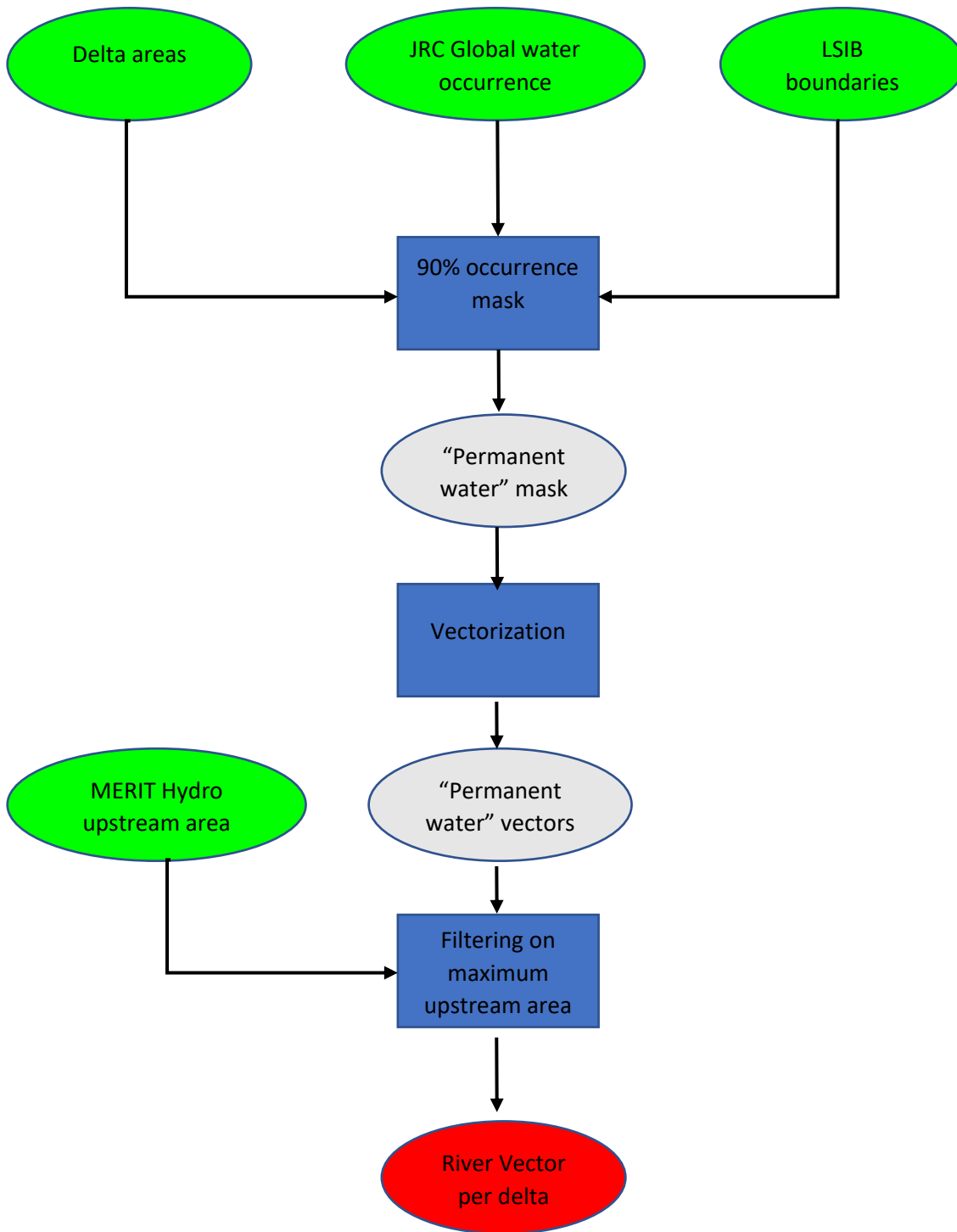


Figure 3.5. Schematic overview of the image processing. In green the input, in blue the operation, in grey the intermediate result and in red the end result.

3.3 Vector processing

The resulting rivers are combined with the sediment flux data from Nienhuis et al. (2020). For vector processing, seven deltas are analysed. This selection is made based on the size of the deltas, connectivity of the main river vector and a low wave sediment flux (Q_{wave}). Deltas where the river is divided into multiple vectors due to the vectorization process, are not taken into account.

A skeleton is made from the rivers using the centerline function. The centerline function reveals the simplified form of each river, or skeleton. The dataset is pruned where there are unreasonably small dangles (1km) or where the other waterbodies were inaccurately clipped from the result. From the pruned skeleton nodes are created on all intersections and end points and divide these nodes into begin, intersection and end nodes. This skeleton is used to get a general overview of the river and all its distributary channels and quantify the number of junctions, forks and outlets and connect this to fluvial and tidal influences.

A schematic overview of the vector processing can be found in figure 3.6.

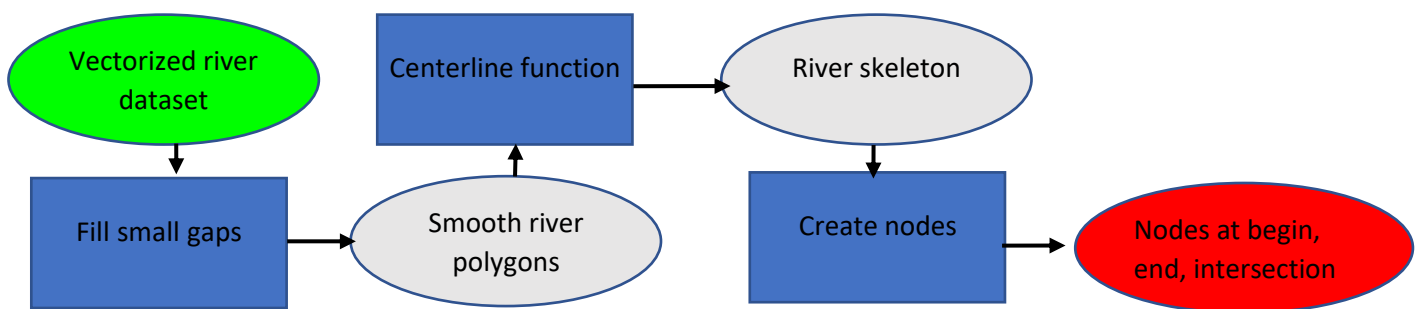


Figure 3.6. Schematic overview of vector processing. In green the input, in blue the operation, in grey the intermediate result and in red the end result.

3.4 Statistics

To place all rivers on a continuous spectrum, a ratio of the fluvial sediment flux (Q_{river}) and the tidal sediment flux (Q_{tide}) is taken, $T = \frac{Q_{\text{tide}}}{Q_{\text{river}}}$, first introduced in Nienhuis et al. (2018). The amount of intersections and end nodes are compared between the different values of T . A theory from Smart & Maruzzi (1971) is used to determine the number of joints and bifurcations. The individual segment lengths between nodes and the bifurcation length, which in this case is the length from the river mouth to the closest bifurcation/intersection point, will be compared as well.

4. Results

In this chapter, the results following the methods described in chapter 3 are presented.

First an overview of the analysed deltas is given together with the sediment fluxes and different types of nodes quantified in this research. After this, the effect of fluvial and tidal sediment fluxes on the structure of a river is analysed. Finally, correlation of river segment count and length versus fluvial and tidal sediment fluxes presented.

After filtering for connectivity and size, seven river networks remain seen in table 4.1. The deltas vary from highly river-dominated (Yenisei) to highly tide-dominated (St. Lawrence). The Amazon is roughly equally tide- and river-dominated. All rivers shown have relatively low wave sediment flux, Q_{wave} .

<i>Delta name</i>	Q_{river} (kg/s)	Q_{tide} (kg/s)	Q_{wave} (kg/s)	T
<i>Amazon</i>	31142,00	30857,36	65,56	0,991
<i>Fly</i>	2585,90	2188,90	689,31	0,846
<i>Lena</i>	5437,90	549,79	92,77	0,101
<i>Mississippi</i>	27284,00	712,61	314,79	0,026
<i>St Lawrence</i>	2514,07	8816,27	4,22	3,507
<i>Yenisei</i>	3416,00	7,57	1,52	0,002
<i>Yukon</i>	3307,60	527,27	92,59	0,159

Table 4.1. Representing used deltas with sediment fluxes, respectively fluvial, tidal and wave, and $T = \frac{Q_{tide}}{Q_{river}}$.

In figure 4.1 you can see the results of the processing of the seven rivers with their nodes. A subdivision has been made between begin nodes, intersections and end nodes for clarity.

In table 4.2 an overview is given on the number of nodes, with a subdivision for junctions, forks and outlets, and recombination factor per river network. A recombination factor of 0 would mean that these rivers would be fragmentized when one segment is deleted, where a recombination factor of 1 means that there are many ways to reconfigure the network without interrupting it. The Amazon and Yenisei both have relatively high nodes and recombination factors. The Mississippi has few nodes and this translates in a small recombination factor, however, this does not seem to be the case for the St. Lawrence, where a low amount of nodes translate in a maximum recombination factor.

<i>Delta name</i>	<i>Nodes</i>	<i>Forks</i>	<i>Junctions</i>	<i>Outlets</i>	<i>Recombination factor (α)</i>
<i>Amazon</i>	41	20	17	4	0,85
<i>Fly</i>	27	13	9	5	0,69
<i>Lena</i>	33	16	10	7	0,63
<i>Mississippi</i>	7	3	1	3	0,33
<i>st. Lawrence</i>	5	2	2	1	1,00
<i>Yenisei</i>	97	48	40	9	0,83
<i>Yukon</i>	15	7	5	3	0,71

Table 4.2. Subdivision of nodes into forks, junctions and outlets and the recombination factor (forks/junctions) per river.

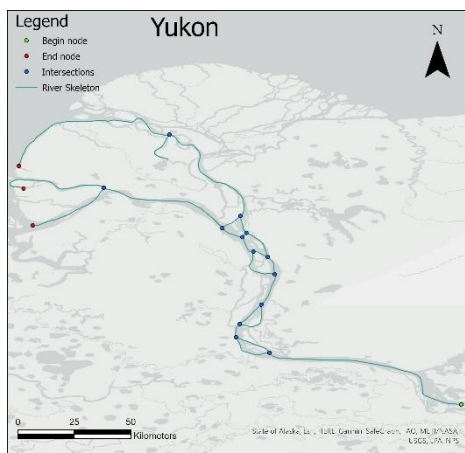
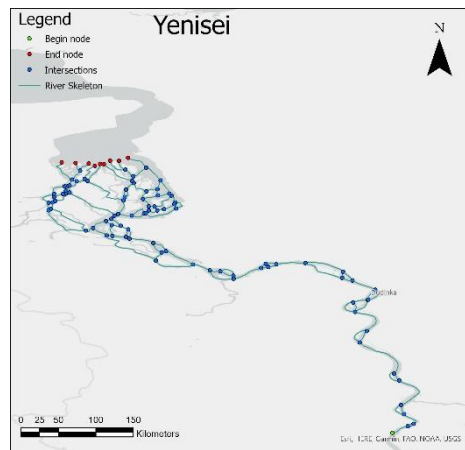
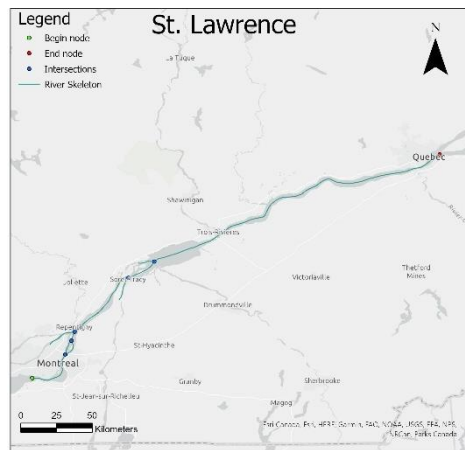
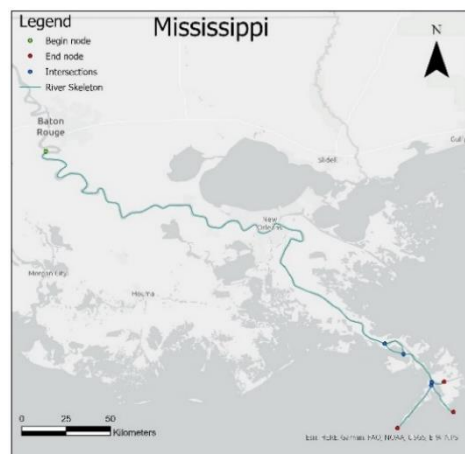
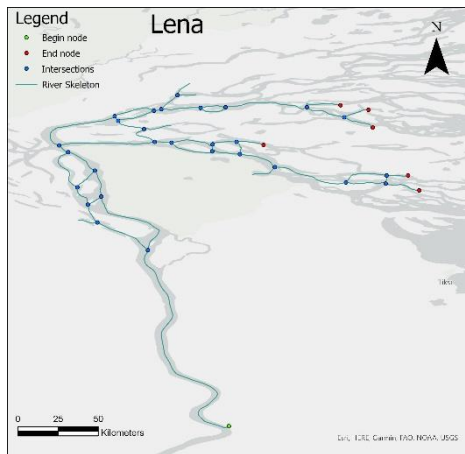
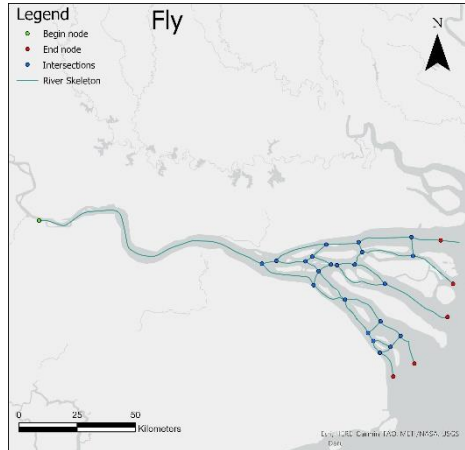
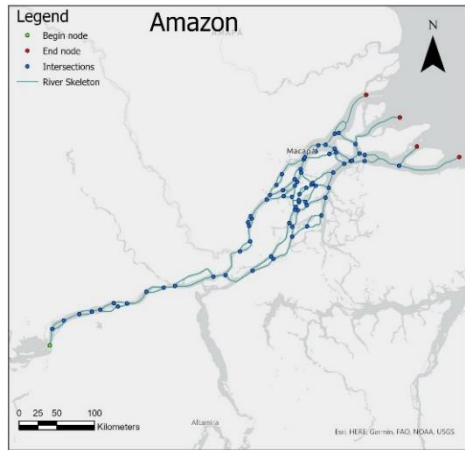


Figure 4.1. Overview of the river networks with the river skeleton and begin (green), end (red) and intersection (blue) nodes.

4.1 Nodes

As can be seen in figure 4.2, the different types of nodes are plotted against the values of $T (= \frac{Q_{\text{tide}}}{Q_{\text{river}}})$ corresponding to the different river networks. In figure 4.2A a bar graph shows the division of total nodes between intersections and end nodes/outlets. The Yenisei appears to have the largest number of nodes as well as the lowest T of 0.002, which translates in mostly river-dominated, where on the other end of the spectrum, St. Lawrence is largely tide dominated with a T of 3.5. With the theory in mind, a decreasing in number and division of nodes would be expected, however, from this figure there does not seem to be a strong correlation. Notably, the Mississippi has very few nodes where the river networks on either side both have more nodes. The Mississippi is more similar to the profile of the St. Lawrence. Comparing the number of nodes to T in figure 4.2B, we see, it is fairly similar to figure 4.2C where the amount of forks, or bifurcations, is compared to T . Both figures have a similar pattern with a slightly downward trend with St. Lawrence having the fewest nodes and bifurcations. Both have a large spread especially around a T of 0.002 and 0.026, Yenisei and Mississippi respectively, with Yenisei having the largest amount of nodes and bifurcations and Mississippi having one of the least. Outlets, or river mouths, have a similar downward trend with increasing T , however, the R^2 is still very low. All node related statistics have a $p > 0.01$. The amount of nodes, junctions and outlets have a $p < 0.05$ with the amount of outlets with the lowest p -value with $p = 0.13$.

4.2 Segments

As can be seen in figure 4.3, the length and number of the river network segments are compared to T . Figure 4.3A shows the mean terminal channel length increasing a lot with a increasing T with a R^2 of 0.94 and $p < 0.05$, where the St. Lawrence has the largest terminal channel length at 165 kilometres and the Lena the smallest terminal channel length at 7 km. In figure 4.3B the amount of segments compared to T are shown. With a R^2 of 0.081, the Yenisei and Amazon are extreme outliers in comparison to the linear regression shown for comparing T with segment count. The mean segment length compared to T in figure 4.3C does not show a significant correlation with a R^2 of 0.062, the extreme outlier being the Mississippi with a calculated mean segment length of 50 kilometres. The correlation between the number of outlets to the terminal channel length is present with an R^2 of 0.45. The comparison of T with segment count, length and number of outlets have a large p value of $p > 0.5$. Comparing T with the terminal channel length resulted in a p value of $p < 0.05$.

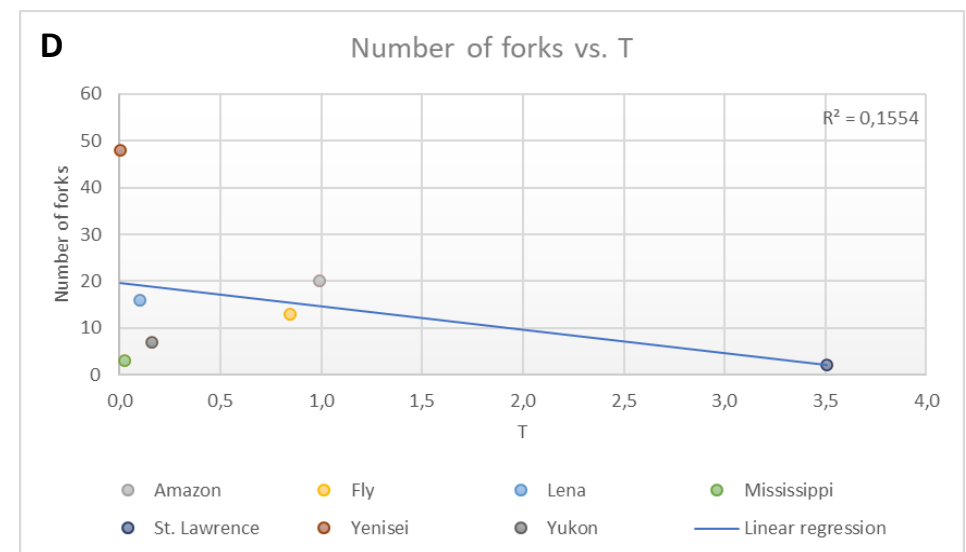
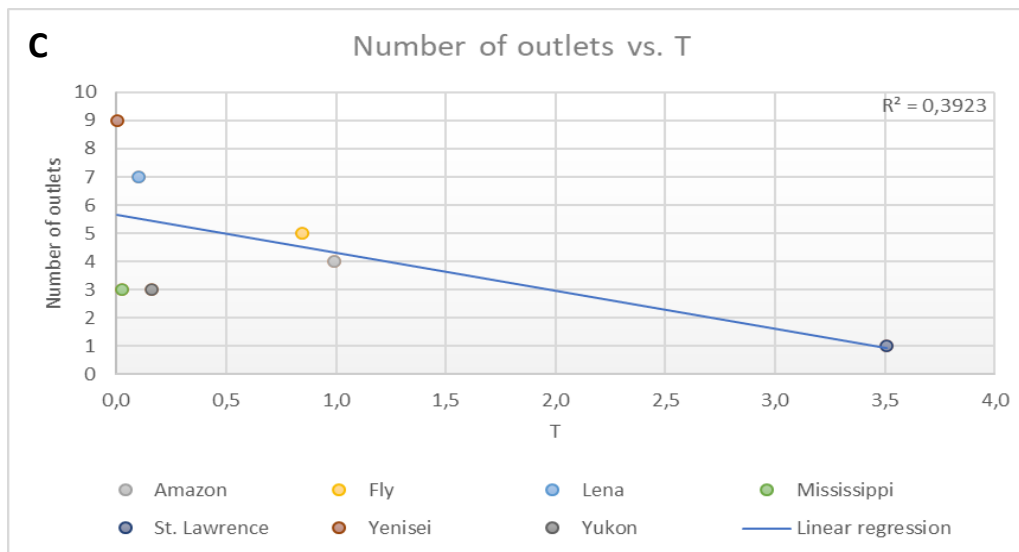
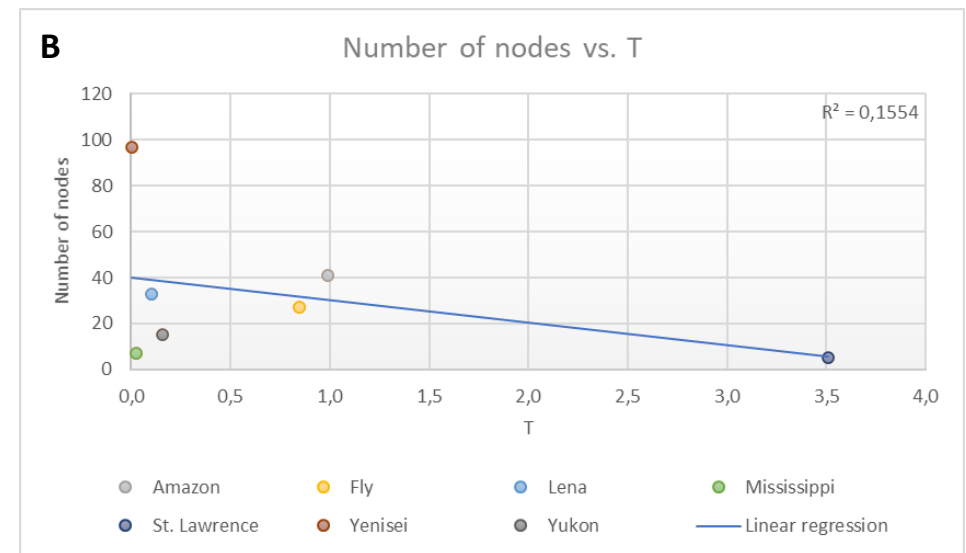
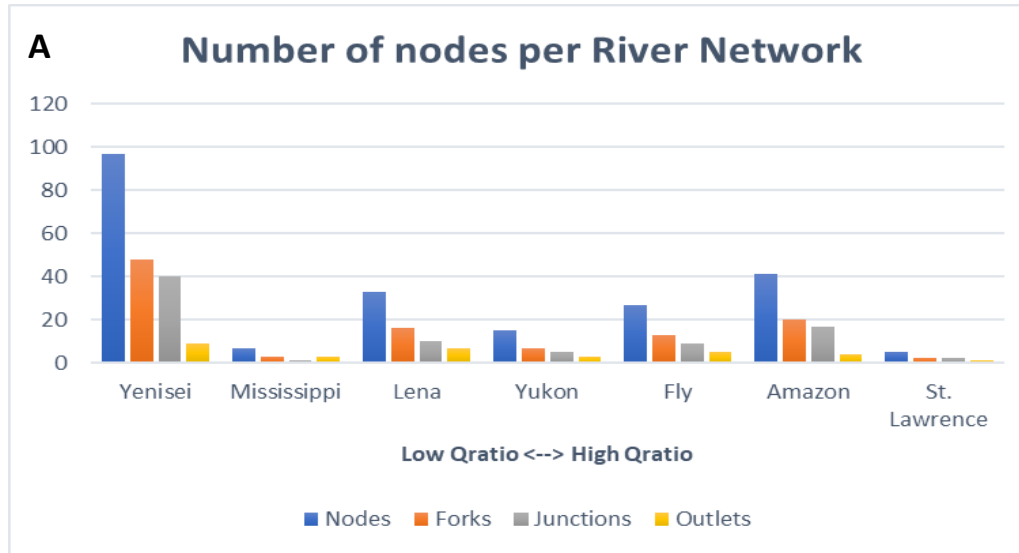


Figure 4.2. A) Subdivision of nodes per river network on an axis of increasing T. B) Number of nodes versus T. C) Number of forks or bifurcations versus T. D) Number of outlets or river mouths versus T. The R² of the linear regression is displayed in the top right corner of each graph.

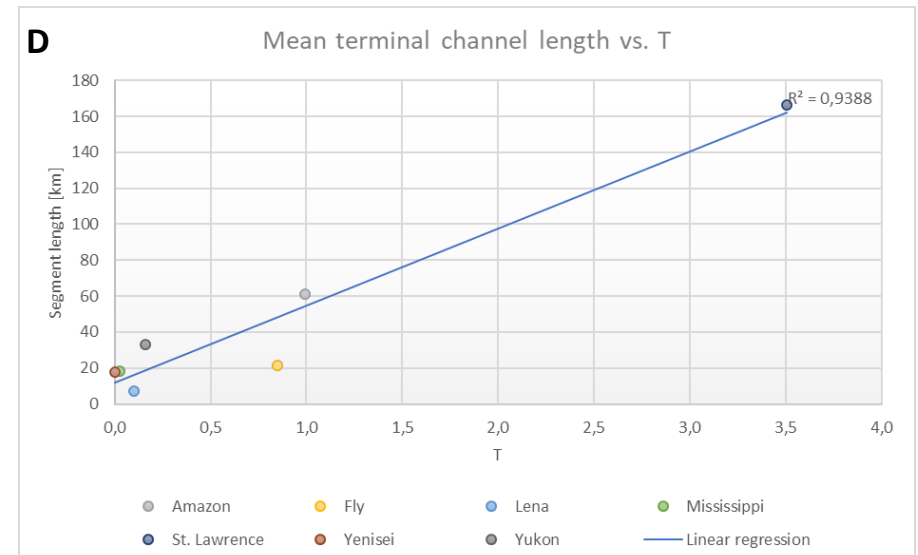
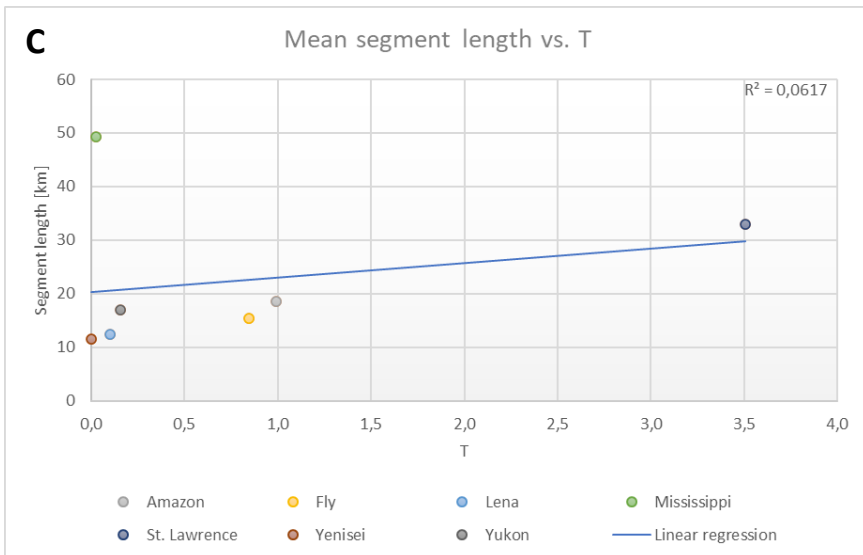
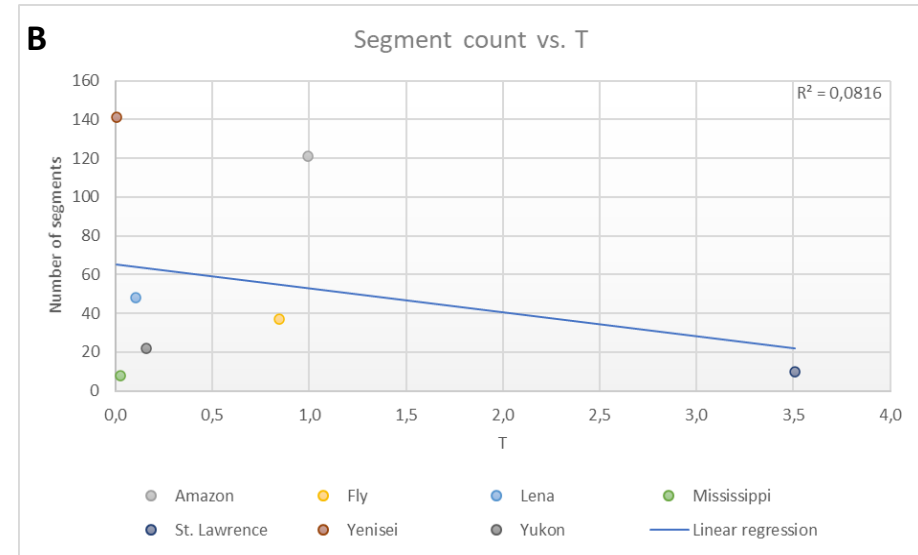
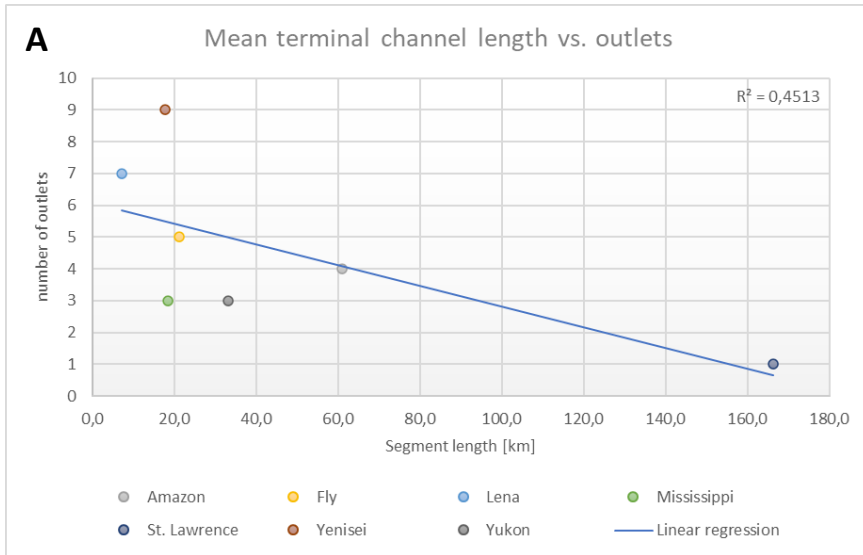


Figure 4.3. A) Mean terminal channel length compared to T. B) Segment count versus T. C) Mean segment length versus T. D) Number of outlets compared to the terminal channel length. The R^2 is displayed in the top or bottom right corner of the graph.

5. Discussion

In this section the results will be discussed. After the discussed results some of the shortcomings are highlighted as well as some of the potential improvements and future applications.

5.1 The effect of tidal and fluvial influence on delta morphology

5.1.1 Nodes

As can be seen from the graphs in figure 4.2, T , the different tidal and fluvial influences do not seem to be a dominant factor in the change in the amount of bifurcations. The highest correlation is outlets compared to T (figure 4.2C) with a R^2 of 0.39 and a $p < 0.05$, which suggests a slight significant relationship that, when the tidal sediment flux increases with respect to the fluvial sediment flux, the number of outlets decreases, which can be explained using the theory of Leonardi et al. (2013). More fluvial sediment causes more rapid mouth-bar creation and build out, so the channels grow relatively fast. Although the bifurcations are more unstable, on the timescale this research is done they are seen as stable channels.

5.1.1.1 Outliers

However, some individual rivers can be highlighted, such as the St. Lawrence, which is extremely tide dominated with a T of 3.5. This river has only one outlet and two forks and junctions, which corresponds to two enclosures (from a fork to junction without interference) (Smart & Moruzzi, 1971). The fact that there are so few nodes in this network can be explained by the lack of sediment through this system, which inhibits the creation of mouth bars (Jerolmack & Swenson, 2007).

Another example of an outlier is the Mississippi river. This river has a relatively low T so fluvial sediment flux is dominant, however the number of bifurcations is below the number of the other river networks that were classified as predominantly fluvial influenced. The Mississippi only has 3 bifurcations, from which one is an enclosure. This gives the Mississippi its recognizable “bird foot” shape. The lack of other bifurcations places the Mississippi on a distinct spot on most of the plots, where it is on the low side of the T spectrum but with deviating values for number of nodes and bifurcations from the other networks.

5.1.2 River segments

As to the segment lengths in the different river networks, it does seem that there is a correlation with tidal and fluvial influences. The terminal channel length has a R^2 of 0.94 and $p < 0.05$ which is significant. This means that the segments closest to the outlet, which are also the newest bifurcations, are decreasing in length with increasing tidal influences. This is consistent with the theory that more sediment causes more frequent bifurcations, which creates a branching pattern with decreasing channel length (Jerolmack & Swenson, 2007). This implies that more bifurcations means shorter terminal channel length. The amount of segments or the mean length of the segments does not seem to have any correlation with the influence of different sediment fluxes. However, this could be due to one or more outliers. For example, looking at figure 5.1, when omitting the Mississippi data, the mean segment length correlation increased significantly. This suggests that first, the segments in a river network do get shorter when fluvial sediment flux is more dominant, which supports Jerolmack & Swenson (2007), and second, the Mississippi is a general outlier where fluvial sediment flux is dominant but the river has relatively few bifurcations.

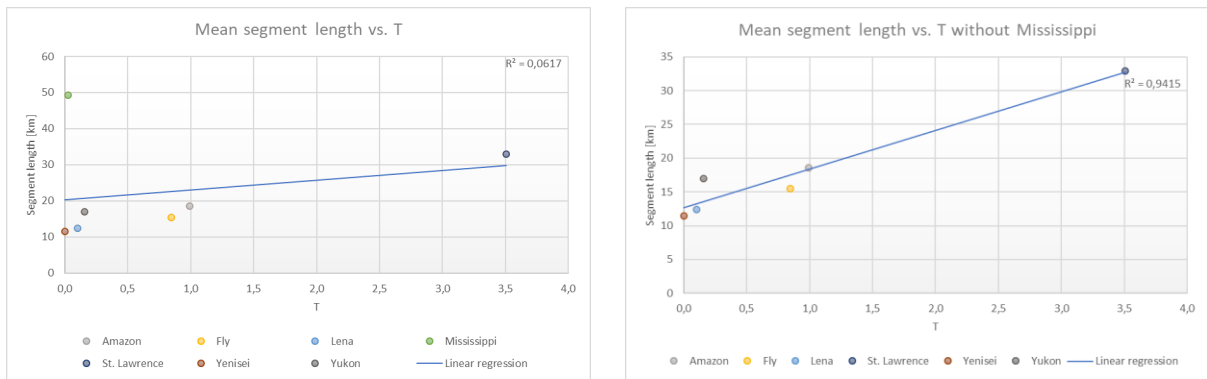


Figure 5.1. Comparison of mean segment length and T for the dataset with Mississippi included (left) and excluded (right).

5.2 Sensitivity

Sensitivity analysis, in the form of omitting one river network at a time from the analysis, shows that each river network has a significant role in the analysis (appendix A). The reader should bear in mind that there are only seven results taken into account, this is because of the selection procedure, mainly the criterium of connectivity. The number of results makes any omission of data rather impactful. The number of results is low and struggles to successfully produce meaningful statistics, the chance on sampling errors is high. Especially the omission of the results for the St. Lawrence network has a big influence on the overall results. Since St. Lawrence is such a outlier, both for T and number of bifurcations, it weighs heavily for each analysis. With only seven results, it could be that any of the seven is an outlier and this could cause uncertainty in any of the results.

5.3 Data quality & improvement

The major shortcoming of this research is mainly the quantity of the results. This can be traced back to the filtering of the water mask for connected water pixels which had the highest flow according to the MERIT Hydro dataset, as can be read in the Methods chapter. Due to the fact that, in the process to extract the main river from the permanent water mask, the pixel size went up from 30 meters to 400 meters and some smaller channels were filtered out. These channels are sometimes the parts that connect multiple bigger channels which in turn caused serious fragmentation of the network. Because of this, only parts of deltas remained which made it impossible to run the rest of the process on those parts. Some of the deltas were still used, they did miss some parts as can be seen in figure 5.2. A useful technique to recognize water bodies could be that of Huang et al. (2018). They used Sentinel-1 SAR (Synthetic Aperture Rader) to extract an automated surface water extent layer. However, this was only tested on two areas so large scale application is not yet proven to work.

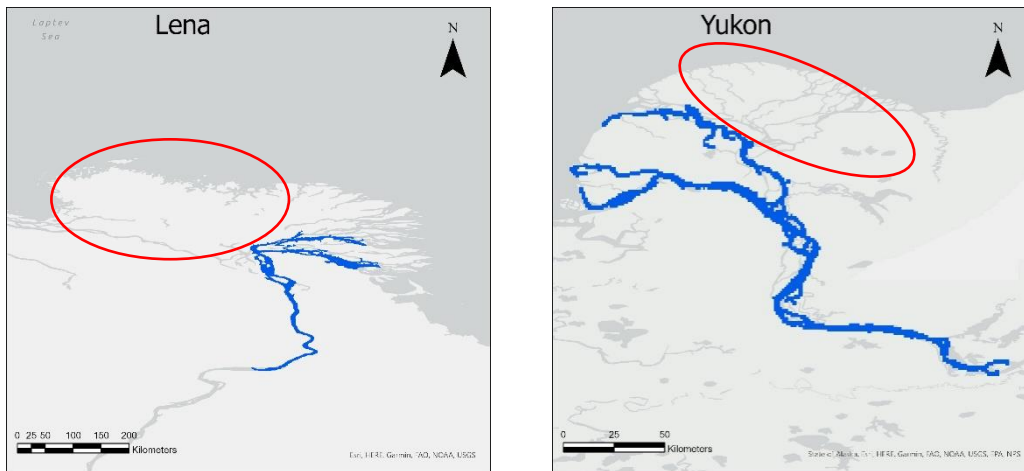


Figure 5.2. Left) in blue the Lena river mask, in red the missing area. Right) in blue the Yukon river mask, in red the missing area.

The large-scale nature of this research asks for a widely applicable and rapid process. This is why the GEE platform was chosen. However, the platform turned out to be ill equipped to handle the processes used in this research, in particular the filtering and vectorization of data. In this research this was accommodated by reducing the number of deltas the selection was used on. The vectorization takes up a large amount of time or cannot complete the operation at all. In future research more attention could be put in creating a sufficient permanent water mask from which the rivers could be extracted. This way the vectorization could be omitted, which would most likely increase the number of river networks present at the end of the process.

Still, using the data and results at hand, we can say something about the overall process by looking at the accuracy of the river networks present. Overall the process to derive a single skeleton and nodes from the images works quite well. Although consecutive floating islands or enclosures are somewhat problematic as can be seen in figure 5.3. The figure highlights two areas which can cause overestimation of the nodes in rivers with lots of small bars. In area figure 5.3 point A, a channel spans laterally between two channels with nodes on both sides. However, this would suggest there are two nodes (junctions or forks) in this part, when it is really only one bifurcation. If such situations occur multiple times in a single network, the number of calculated intersections can increase significantly, which in turn can affect overall results. The same goes for figure 5.3 point B. Here there are two consecutive bars with a small area in between, the segment in between both intersections is very small. When this happens multiple times in a single network it can skew the number and mean length of the segments.

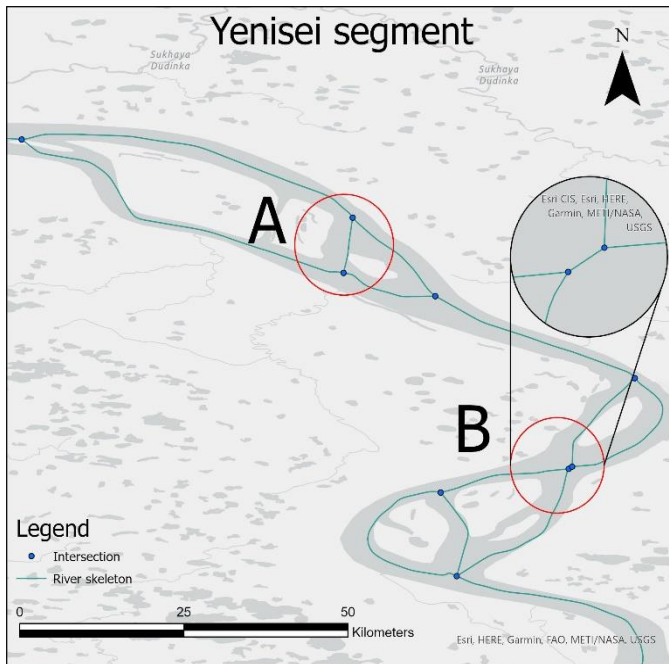


Figure 5.3. Segment of the Yenisei river displaying flaws in the skeletonization process.

5.4 Future research

The results from this study may not be applicable right away, but with several improvements the large scale quantification of effects on delta morphology can be very interesting. As mentioned above, the study would benefit hugely from an improved permanent water mask and/or a way to extract the river in such a way that the shape of the original river network remains. The Google Earth Engine platform is promising to extract the necessary data on large scale, however a different way to extract the river mask is needed. Data on river networks can help in calibrating different kinds of hydrological models.

To improve this study and obtain a reliable result and to quantify the influence of sediment fluxes on for example bifurcations an increase in datapoints is necessary. This can be done by improving the image processing. A better water mask could reduce fragmentation of the main river, this can also help extracting the main river from all water bodies.

Besides the increasing of datapoints, the vector processing could improve as well. As can be seen in figure 5.3, the skeleton and therefore the network nodes are not consistent. This has been partly done manually in this research however it would benefit greatly of an automated approach.

Once the size of the dataset is increased and the skeleton and nodes represent reality, this study can be quite useful. The results could help better predict how changes in sediment fluxes affect delta morphology, for example what happens when the fluvial sediment is reduced due to a dam and tidal fluxes stay the same. Since almost a quarter of the population lives in delta areas, changes in river patterns could be devastating for the people living from and around the water of the river.

For now, no global data on distributary networks exist. The product derived from this study could fill this gap once the aforementioned flaws are fixed. Such networks could be useful calibrating hydrological models, for example, sediment transport is divided between river mouths. Global knowledge of the number of river mouths at a given delta could help improve models using variables influenced by the number of river outlets.

6. Conclusion

In this research the influence of fluvial or tidal dominance on a river network was quantified. The results were in line with some of the previous findings on the scaling relationships in deltas and influences on delta morphology. The more a river delta is dominated by the fluvial sediment flux, the more outlets a network has and with increasing amount of outlets, the terminal channel length decreases. This follows the stated hypotheses and literature found. More fluvial sediment causes more rapid mouth-bar creation and build out, so the channels grow relatively fast. Although the bifurcations are more unstable, on the timescale this research is done they are seen as stable channels. Number of bifurcations had a very weak correlation to the change in tidal and fluvial sediment flux. The reader has to keep in mind that these results were achieved using only seven deltas, which makes the result susceptible to outliers and errors. Although the process works, the output has much room to improve. Future research could improve the quality of the input water mask and streamline the used processes whilst keeping the large-scale nature of the research which is not yet successfully achieved anywhere else. The result of such a study could be used for calibration of (hydrological) models and can help predict the influence of human impact on delta morphology in a quantifiable way.

For now, a dataset of global distributary networks is not yet available. This study lays the groundwork for such a dataset and provides some suggestions for improving the data processing. Knowing how and how much the influences of fluvial and tidal sediment fluxes shape the river network can be of great importance. Sudden changes in the delta area can be devastating for the people living there, this study could determine if there is an environment where, with a slight disturbance, such changes can occur.

Bibliography

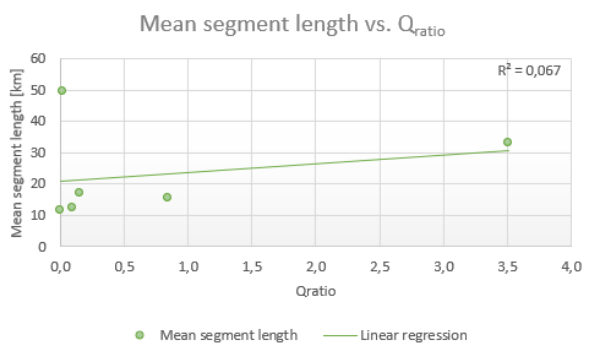
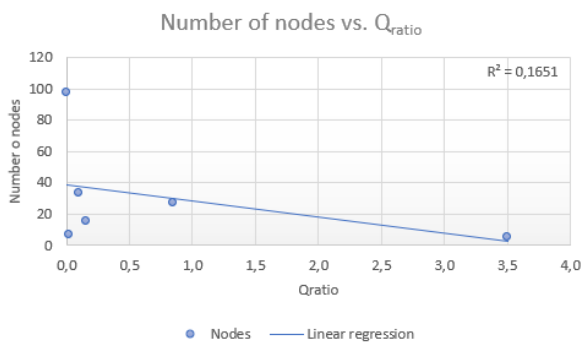
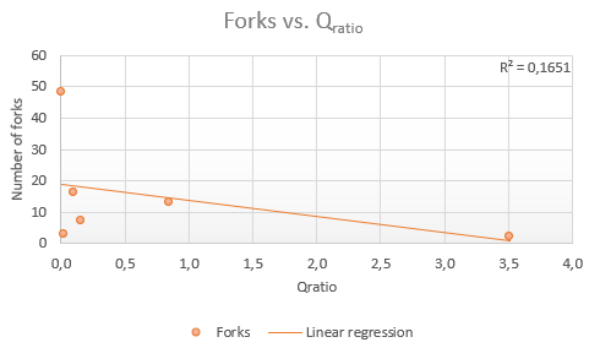
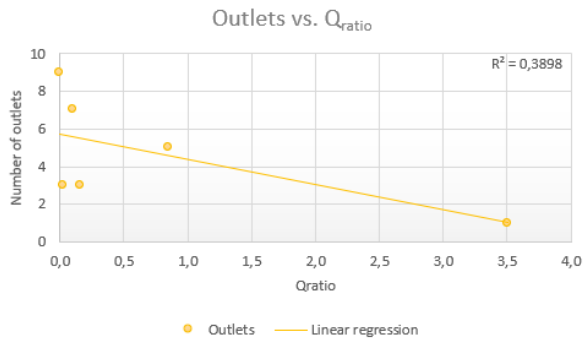
- Bates, C. G., & Freeman, Jr., J. C. (1953). Inter-Relations Between Jet Behavior and Hydraulic Processes Observed At Deltaic River Mouths and Tidal Inlets. *Coastal Engineering Proceedings*, 1(3), 12. <https://doi.org/10.9753/icce.v3.12>
- Carson, M. A., & Kirby, M. J. (1972). Hillslope Form and Process: By MA Carson, ... and Mf Kirkby. The University Press.
- Cohen, S., Kettner, A. J., & Syvitski, J. P. M. (2014). Global suspended sediment and water discharge dynamics between 1960 and 2010: Continental trends and intra-basin sensitivity. *Global and Planetary Change*, 115, 44–58. <https://doi.org/10.1016/j.gloplacha.2014.01.011>
- Edmonds, D. A., & Slingerland, R. L. (2007). Mechanics of river mouth bar formation: Implications for the morphodynamics of delta distributary networks. *Journal of Geophysical Research: Earth Surface*, 112(2), 1–14. <https://doi.org/10.1029/2006JF000574>
- Egbert, G. D., & Erofeeva, S. Y. (2002). Efficient inverse modeling of barotropic ocean tides. *Journal of Atmospheric and Oceanic Technology*, 19(2), 183–204. [https://doi.org/10.1175/1520-0426\(2002\)019<0183:EIMOBO>2.0.CO;2](https://doi.org/10.1175/1520-0426(2002)019<0183:EIMOBO>2.0.CO;2)
- Elliot, T. (1986). *Sedimentary environments and facies*. Oxford: Blackwell Scientific.
- Foufoula-Georgiou, E. (2013). A vision for a coordinated international effort on delta sustainability. *IAHS-AISH Proceedings and Reports*, 358(July), 3–11.
- Galloway, W. E. (1975). Process Framework for Describing the Morphologic and Stratigraphic Evolution of Deltaic Depositional Systems, (September).
- Gorelick, N., Hancher, M., Dixon, M., Ilyushchenko, S., Thau, D., & Moore, R. (2017). Remote Sensing of Environment Google Earth Engine : Planetary-scale geospatial analysis for everyone. *Remote Sensing of Environment*, 202, 18–27. <https://doi.org/10.1016/j.rse.2017.06.031>
- Huang, W., DeVries, B., Huang, C., Lang, M. W., Jones, J. W., Creed, I. F., & Carroll, M. L. (2018). Automated extraction of surface water extent from Sentinel-1 data. *Remote Sensing*, 10(5), 1–18. <https://doi.org/10.3390/rs10050797>
- Islam, M. R., Miah, M. G., & Inoue, Y. (2016). Analysis of Land use and Land Cover Changes in the Coastal Area of Bangladesh using Landsat Imagery. *Land Degradation and Development*, 27(4), 899–909. <https://doi.org/10.1002/ldr.2339>
- Iwantoro, A. P., Van Der Vegt, M., & Kleinhans, M. G. (2020). Morphological evolution of bifurcations in tide-influenced deltas. *Earth Surface Dynamics*, 8(2), 413–429. <https://doi.org/10.5194/esurf-8-413-2020>
- Jerolmack, D. J. (2009). Conceptual framework for assessing the response of delta channel networks to Holocene sea level rise. *Quaternary Science Reviews*, 28(17–18), 1786–1800. <https://doi.org/10.1016/j.quascirev.2009.02.015>
- Jerolmack, D. J., & Swenson, J. B. (2007). Scaling relationships and evolution of distributary networks on wave-influenced deltas. *Geophysical Research Letters*, 34(23), 1–5. <https://doi.org/10.1029/2007GL031823>
- Kästner, K., Hoitink, A. J. F., Vermeulen, B., Geertsema, T. J., & Ningsih, N. S. (2017). Distributary channels in the fluvial to tidal transition zone. *Journal of Geophysical Research: Earth Surface*, 122(3), 696–710. <https://doi.org/10.1002/2016JF004075>
- Kleinhans, M. G., Ferguson, R. I., Lane, S. N., & Hardy, R. J. (2013). Splitting rivers at their seams:

- Bifurcations and avulsion. *Earth Surface Processes and Landforms*, 38(1), 47–61.
<https://doi.org/10.1002/esp.3268>
- Kuenzer, C., Klein, I., Ullmann, T., Georgiou, E. F., Baumhauer, R., & Dech, S. (2015). Remote sensing of river delta inundation: Exploiting the potential of coarse spatial resolution, temporally-dense MODIS time series. *Remote Sensing*, 7(7), 8516–8542. <https://doi.org/10.3390/rs70708516>
- Leonardi, N., Canestrelli, A., Sun, T., & Fagherazzi, S. (2013). Effect of tides on mouth bar morphology and hydrodynamics. *Journal of Geophysical Research: Oceans*, 118(9), 4169–4183.
<https://doi.org/10.1002/jgrc.20302>
- Nienhuis, J. H., Ashton, A. D., Edmonds, D. A., Hoitink, A. J. F., Kettner, A. J., Rowland, J. C., & Törnqvist, T. E. (2020). Global-scale human impact on delta morphology has led to net land area gain. *Nature*, 577(7791), 514–518. <https://doi.org/10.1038/s41586-019-1905-9>
- Nienhuis, Jaap H., Hoitink, A. J. F. T., & Törnqvist, T. E. (2018). Future Change to Tide-Influenced Deltas. *Geophysical Research Letters*, 45(8), 3499–3507.
<https://doi.org/10.1029/2018GL077638>
- North, C. P., & Warwick, G. L. (2007). Fluvial fans: Myths, misconceptions, and the end of the terminal-fan model. *Journal of Sedimentary Research*, 77(9–10), 693–701.
<https://doi.org/10.2110/jsr.2007.072>
- Olariu, C., & Bhattacharya, J. P. (2006). Terminal distributary channels and delta front architecture of river-dominated delta systems. *Journal of Sedimentary Research*, 76(2), 212–233.
<https://doi.org/10.2110/jsr.2006.026>
- Pekel, J. F., Cottam, A., Gorelick, N., & Belward, A. S. (2016). High-resolution mapping of global surface water and its long-term changes. *Nature*, 540(7633), 418–422.
<https://doi.org/10.1038/nature20584>
- Roberts, H. H. (1997). Dynamic changes of the Holocene Mississippi River delta plain: The delta cycle. *Journal of Coastal Research*, 13(3), 605–627.
- Roelvink, J. A. and Van Banning, G. K. F. M. (1995). Design and development of DELFT3D and application to coastal morphodynamics. *Oceanographic Literature Review*, 42(11), 925.
- Shaw, J. B., & Mohrig, D. (2014). The importance of erosion in distributary channel network growth, Wax Lake Delta, Louisiana, USA. *Geology*, 42(1), 31–34. <https://doi.org/10.1130/G34751.1>
- Smart, J. S., & Moruzzi, V. L. (1971). Quantitative Properties of Delta Channel Networks, 27. Retrieved from <http://oai.dtic.mil/oai/oai?verb=getRecord&metadataPrefix=html&identifier=AD0719918>
- Smith, N. D., & Rogers, J. (1999). *Fluvial Sedimentology VI. Fluvial Sedimentology VI*.
<https://doi.org/10.1002/9781444304213>
- Syvitski, J. P. M. (2008). Deltas at risk. *Sustainability Science*, 3(1), 23–32.
<https://doi.org/10.1007/s11625-008-0043-3>
- Tejedor, A., Longjas, A., Caldwell, R., Edmonds, D. A., Zaliapin, I., & Fofoula-Georgiou, E. (2016). Quantifying the signature of sediment composition on the topologic and dynamic complexity of river delta channel networks and inferences toward delta classification. *Geophysical Research Letters*, 1–8. <https://doi.org/10.1002/2016GL068210>.Received
- Tejedor, A., Longjas, A., Zaliapin, I., & Fofoula-Georgiou, E. (2015). Delta channel networks: 1. A graph-theoretic approach for studying connectivity and steady state transport on deltaic surfaces. *Journal of the American Water Resources Association*, 5(3), 2–2.
<https://doi.org/10.1111/j.1752-1688.1969.tb04897.x>

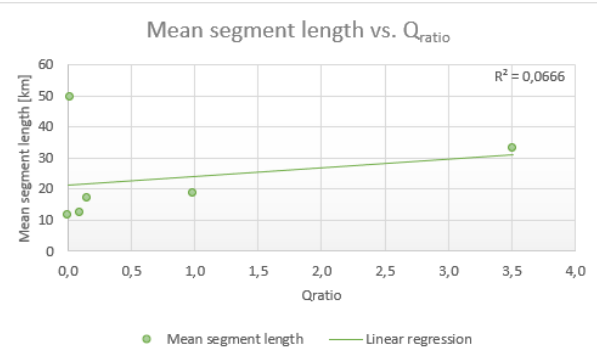
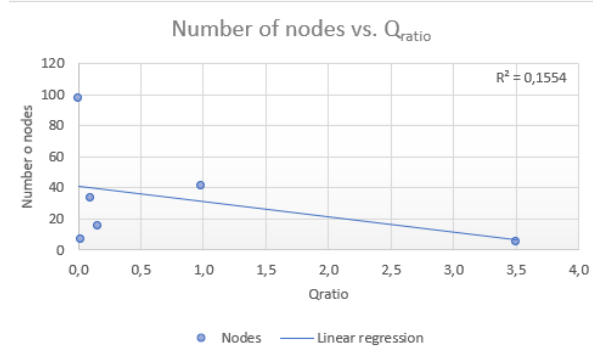
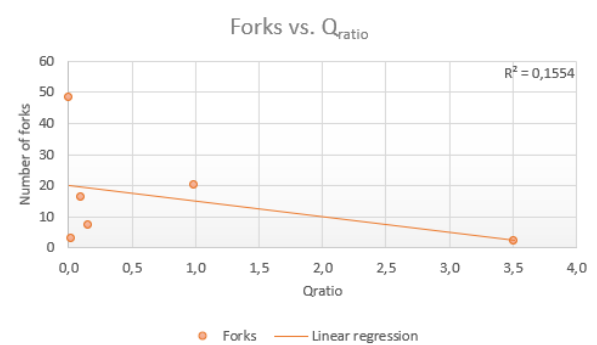
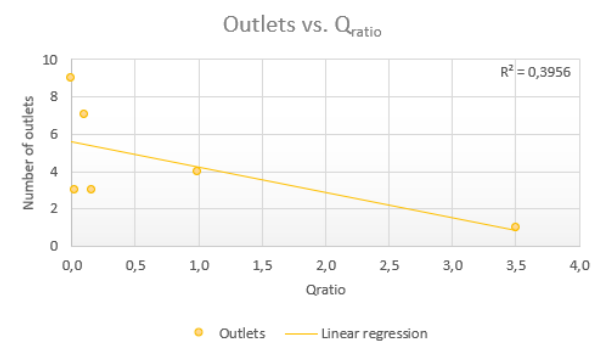
- Wright, L. D. (1977). Sediment transport and deposition at river mouths: A synthesis. *Bulletin of the Geological Society of America*, 88(6), 857–868. [https://doi.org/10.1130/0016-7606\(1977\)88<857:STADAR>2.0.CO;2](https://doi.org/10.1130/0016-7606(1977)88<857:STADAR>2.0.CO;2)
- Wright, L. D., & Coleman, J. M. (1974). Mississippi River Mouth Processes: Effluent Dynamics and Morphologic Development. *The Journal of Geology*, 82(6), 751–778. <https://doi.org/10.1086/628028>
- Wu, Q., Lane, C. R., Li, X., Zhao, K., Zhou, Y., Clinton, N., ... Lang, M. W. (2019). Integrating LiDAR data and multi-temporal aerial imagery to map wetland inundation dynamics using Google Earth Engine. *Remote Sensing of Environment*, 228(September 2018), 1–13. <https://doi.org/10.1016/j.rse.2019.04.015>
- Xue Liangqing, & Galloway, W. E. (1991). Fan-Delta, Braid Delta and the Classification of Delta Systems. *Acta Geologica Sinica - English Edition*, 4(4), 387–400. <https://doi.org/10.1111/j.1755-6724.1991.mp4004004.x>
- Yamazaki, D., Ikeshima, D., Sosa, J., Bates, P. D., Allen, G. H., & Pavelsky, T. M. (2019). MERIT Hydro: A High-Resolution Global Hydrography Map Based on Latest Topography Dataset. *Water Resources Research*, 55(6), 5053–5073. <https://doi.org/10.1029/2019WR024873>

Appendix – A Sensitivity analysis

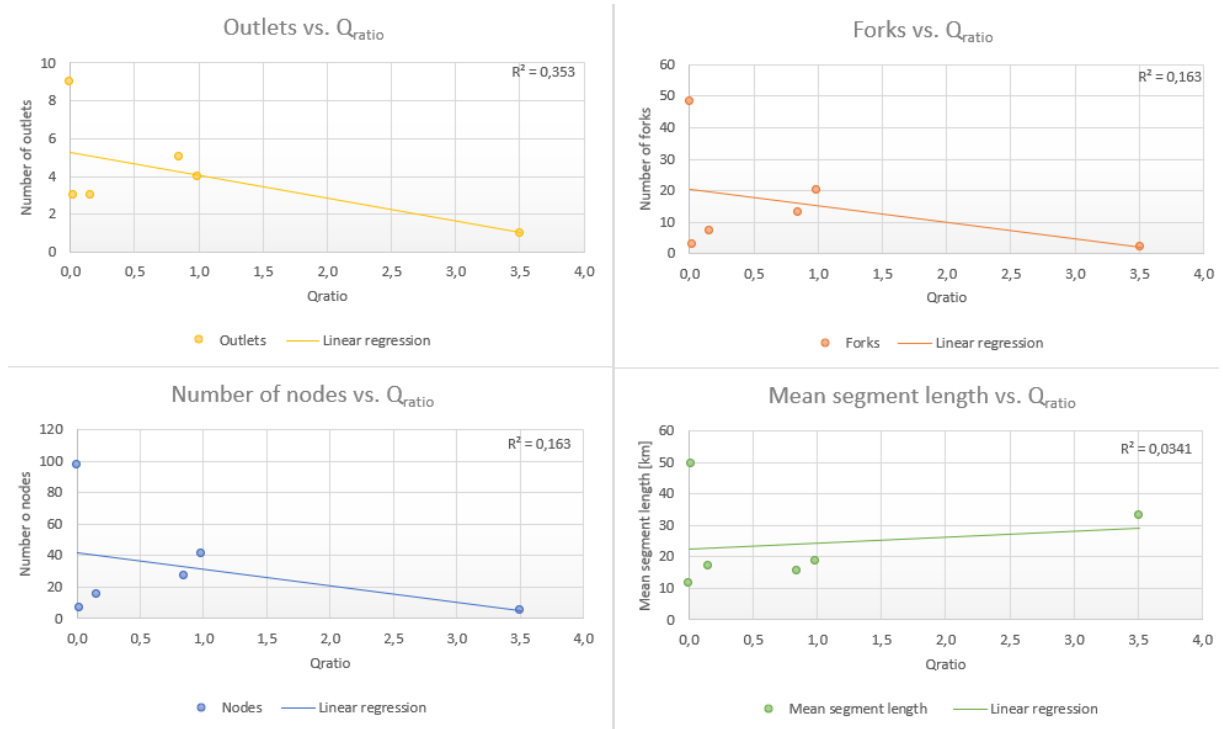
1. Data without Amazon



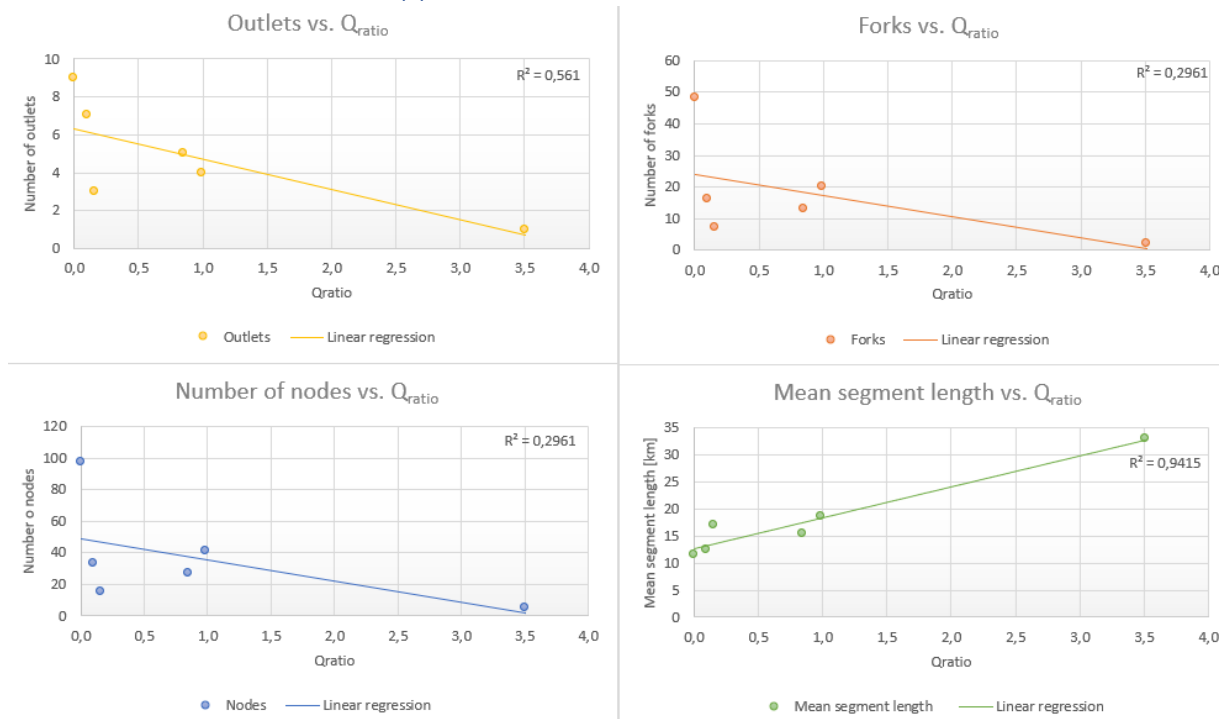
2. Data without Fly



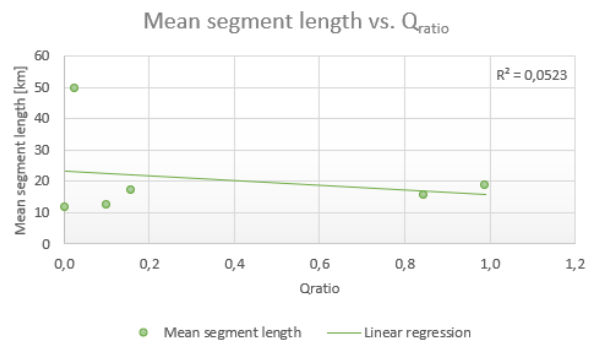
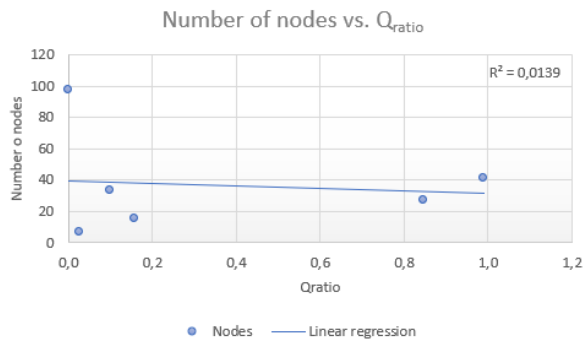
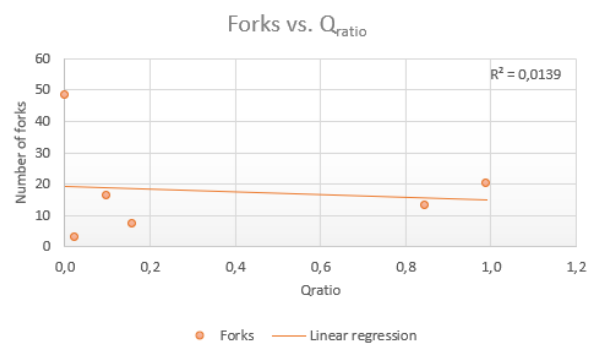
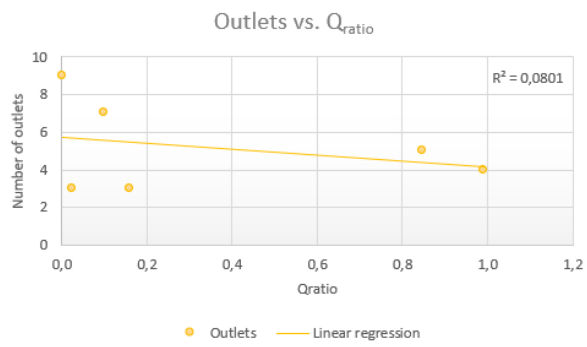
3. Data without Lena



4. Data without Mississippi

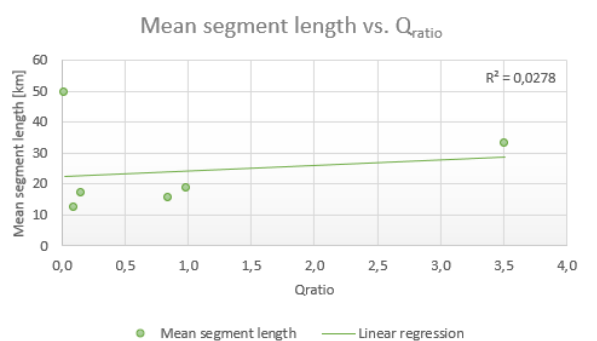
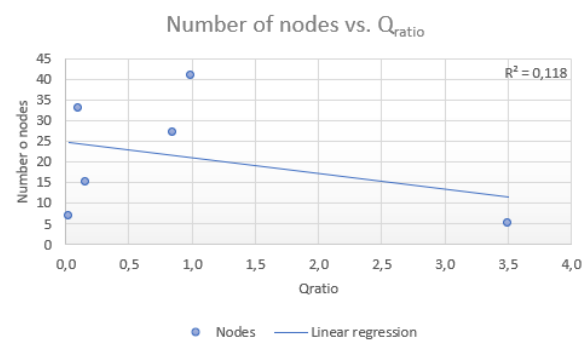
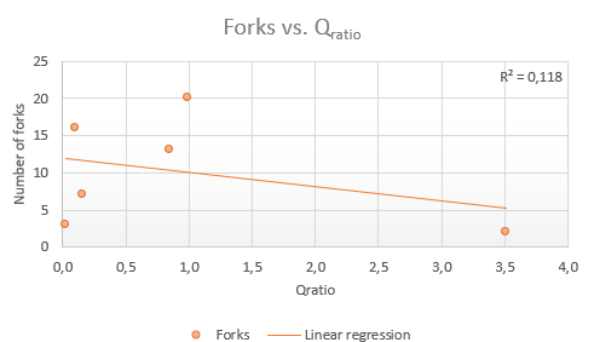


5. Data without St. Lawrence



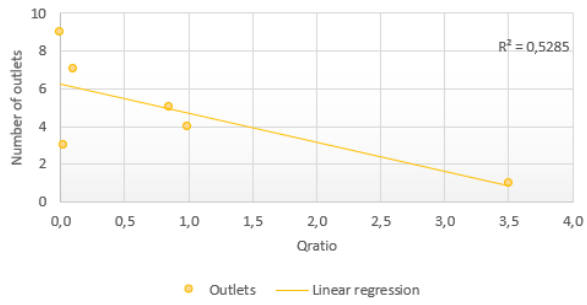
*note: the x-axis is different from the other graphs

6. Data without Yenisei

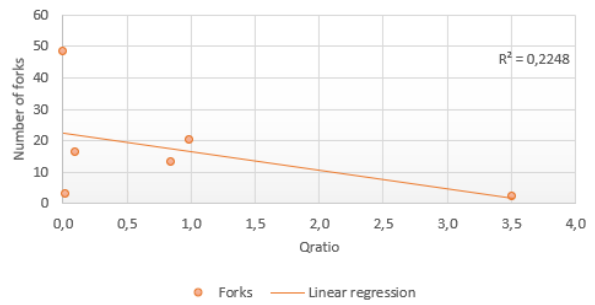


7. Data without Yukon

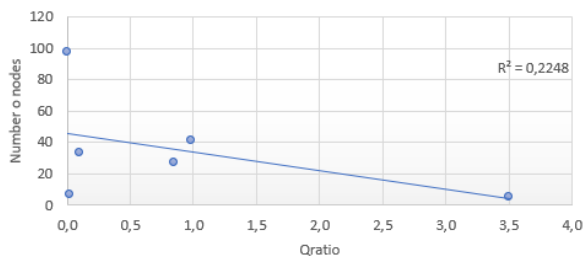
Outlets vs. Q_{ratio}



Forks vs. Q_{ratio}



Number of nodes vs. Q_{ratio}



Mean segment length vs. Q_{ratio}

